Available online at www.sciencedirect.com
ScienceDirect
Expert Systems with Applications 34 (2008) 2039–2048
Expert Systems with Applications
www.elsevier.com/locate/eswa

Artificial immune recognition system with fuzzy resource allocation mechanism classifier, principal component analysis and FFT method based new hybrid automated identification system for classification of EEG signals

Kemal Polat *, Salih Güneş

Selcuk University, Department of Electrical and Electronics Engineering, 42075 Konya, Turkey

Abstract

The aim of this study is to classification of EEG signals using a new hybrid automated identification system based on Artificial immune recognition system (AIRS) with fuzzy resource allocation mechanism, principal component analysis (PCA) and fast Fourier transform (FFT) method. EEG signals used belong to normal subject and patient that has epileptic seizure. The proposed system has three stages: (i) feature extraction using Welch (FFT) method, (ii) dimensionality reduction using PCA, and (iii) EEG classification using AIRS with fuzzy resource allocation. We have used the 10-fold cross-validation, classification accuracy, sensitivity and specificity analysis, and confusion matrix to show the robustness and efficient of proposed system. The obtained classification accuracy is about 100% and it is very promising compared to the previously reported classification techniques.

Keywords: EEG signals; Artificial immune recognition system; Fuzzy resource allocation mechanism; Welch method; Principal component analysis; Expert systems

1. Introduction

The brain is a highly complex system. Understanding the behavior and dynamics of billions of interconnected neurons from the brain signal requires knowledge of several signal-processing techniques, from the linear and nonlinear domains, and its correlation to the physiological events. Many investigators, for example, Duke and Pritchard (1991), has proved that complex dynamical evolutions lead to chaotic regimes. In the last 30 years, experimental observations have pointed out that, in fact, chaotic systems are common in nature. A detail of such system is given by Boccaletti, Grebogi, Lai, Mancini, and Mazaet (2000). In theoretical modeling of neural systems, emphasis has been put mainly on either stable or cyclic behaviors. Perhaps studying the chaotic behavior at neural level could help in identifying schizophrenia, insomnia, epilepsy and other disorders (Glass, Michel, Mackey, & Shrier, 1983; Jaeseung, Jeong-Ho, Kim, & Seol-Heui, 2001; Philippe & Henri, 2001; Kannathal, Choo, Rajendra Acharya, & Sadasivana, 2005).

The electroencephalogram (EEG) signal is widely used clinically to investigate brain disorders. The study of the brain electrical activity, through the electroencephalographic records, is one of the most important tools for the diagnosis of neurological diseases (Adeli, Zhou, & Dadmehr, 2003; Hazarika, Chen, Tsoi, & Sergejew, 1997; Rosso, Figliola, Creso, & Serrano, 2004). Large amounts of data are generated by EEG monitoring systems for electroencephalographic changes, and their complete visual analysis is not routinely possible. Computers have long been proposed to solve this problem and thus, automated

* Corresponding author.
E-mail addresses: kpolat@selcuk.edu.tr (K. Polat), sgunes@selcuk.edu.tr (S. Güneş).

0957-4174/$ - see front matter © 2007 Elsevier Ltd. All rights reserved.
doi:10.1016/j.eswa.2007.02.009

systems to recognize electroencephalographic changes have been under study for several years (Gabor & Seyal, 1992; Glover, Raghaven, Ktonas, & Frost, 1989; Nigam & Graupe, 2004; Webber, Litt, Lesser, Fisher, & Bankman, 1993). There is a strong demand for the development of such automated devices, due to the increased use of prolonged and long-term video EEG recordings for proper evaluation and treatment of neurological diseases and prevention of the possibility of the analyst missing (or misreading) information (Guler & Ubeyli, 2005; Webber et al., 1993).

Having so many factors to analyze to diagnose the epileptic seizure of a patient makes the physician's job difficult. A physician usually makes decisions by evaluating the current test results of a patient and by referring to the previous decisions she made on other patience with the same condition. The former method depends strongly on the physician's knowledge. On the other hand, the latter depends on the physician's experience to compare her patient with her earlier patients. This job is not easy considering the number of factors she has to evaluate. In this crucial step, she may need an accurate tool that lists her previous decisions on the patient having same (or close to same) factors.

Motivated by the need of such an important classification method, in this study, we propose a method to classification of EEG signals. The proposed system has three stages: (i) feature extraction using Welch (FFT) method, (ii) dimensionality reduction using PCA, and (iii) EEG classification using AIRS with fuzzy resource allocation. First, we applied the FFT based Welch spectral analysis method to the EEG signals and we obtained 129 features (attributes) from FFT based Welch method. Second, we used PCA method to reduction from 129 to 5 features. And finally we used AIRS with fuzzy resource allocation as classifier to classification of EEG signals. We obtained 100% classification accuracy via 10-fold cross-validation on the classification of EEG signals. To the best of our knowledge, this classification accuracy is the highest so far.

The remaining of the paper is organized as follows. We present the related work in relation to EEG classification in Section 2. We give the natural and artificial immune system in the next section. In Section 4, we present the recording EEG Data used in experimental studies. We present the proposed system with subsections in Section 5. In Section 6, we give the experimental data to show the effectiveness of our method. Finally, we conclude this paper in Section 7 with future directions.

2. Related work

Classification systems have been used for EEG signals classification problem as for other clinical diagnosis problems. There have been several studies reported focusing on EEG signals classification. These studies applied different methods to the given problem and achieved high classification accuracies using the dataset taken from Andrzejak et al. (2001). Among these studies, Guler, Ubeyli, and Guler (2005) obtained 96.79% classification accuracy using Recurrent neural networks while Kannathal et al. (2005) obtained 95% classification accuracy using ANFIS classifier on the EEG signals classification. While Subasi (2007) reached to 95% classification accuracy using Wavelet and Mixture of experts, 93.6% classification accuracy was obtained using Wavelet and MLPNN. Guler and Ubeyli (2005) obtained 98.68% classification accuracy using Wavelet and ANFIS classifier. In this work, we obtained 100% classification accuracy using 10-fold cross-validation.

3. Natural and artificial immune systems

The natural immune system is a distributed novel-pattern detection system with several functional components positioned in strategic locations throughout the body. Immune system regulates defense mechanism of the body by means of innate and adaptive immune responses. Between these, adaptive immune response is much more important for us because it contains metaphors like recognition, memory acquisition, diversity, self-regulation, etc. The main architects of adaptive immune response are lymphocytes, which can be divided into two classes as T and B lymphocytes (cells), each having its own function. Especially B cells have a great importance because of their secreted antibodies (Abs) that take very critical roles in adaptive immune response.

Artificial Immune Systems emerged in the 1990s as a new computational research area. Artificial Immune Systems link several emerging computational fields inspired by biological behavior such as Artificial Neural Networks and Artificial Life. In the studies conducted in the field of AIS, B cell modeling is the most encountered representation type. Different representation methods have been proposed in that modeling. Among these, shape-space representation is the most commonly used one (De Castro & Timmis, 2002).

The shape-space model (S) aims at quantitatively describing the interactions among antigens (Ags), the foreign elements that enter the body like microbe, etc., and antibodies (Ag-Ab). The set of features that characterize a molecule is called its *generalized shape*. The Ag-Ab representation (binary or real-valued) determines a distance measure to be used to calculate the degree of interaction between these molecules. Mathematically, the generalized shape of a molecule (m), either an antibody or an antigen, can be represented by a set of coordinates $m = \langle m_1, m_2, \ldots, m_L \rangle$, which can be regarded as a point in an L-dimensional real-valued shape-space ($m \in S^L$). In this work, we used real strings to represent the molecules. Antigens and antibodies are considered to be the same length L. The length and cell representation depend upon the given problem (Şahan, Kodaz, Güneş, & Polat, 2004).

4. Recording EEG data

We used the publicly available data described in Andrzejak et al. (2001). In this section, we restrict ourselves

to only a short description and refer to Andrzejak et al. (2001) for further details. The complete data set consists of five sets (denoted A–E) each containing 100 single channel EEG segments. These segments were selected and cut out from continuous multi-channel EEG recordings after visual inspection for artifacts, e.g., due to muscle activity or eye movements. Sets A and B consisted of segments taken from surface EEG recordings that were carried out on five healthy volunteers using a standardized electrode placement scheme (Fig. 1). Volunteers were relaxed in an awake state with eyes open (A) and eyes closed (B), respectively. Sets C, D, and E originated from EEG archive of presurgical diagnosis. EEGs from five patients were selected, all of whom had achieved complete seizure control after resection of one of the hippocampal formations, which was therefore correctly diagnosed to be the epileptogenic zone. Segments in set D were recorded from within the epileptogenic zone, and those in set C from the hippocampal formation of the opposite hemisphere of the brain.

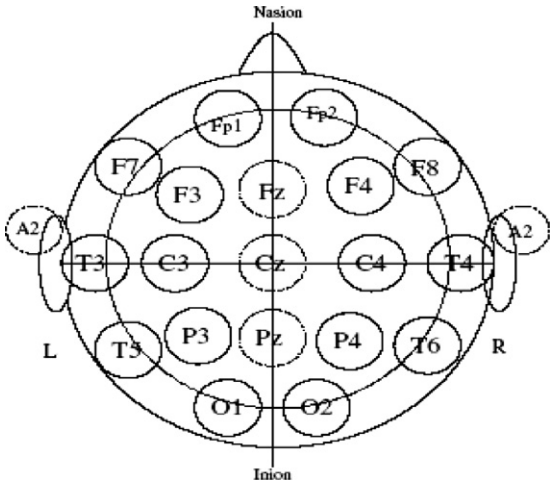

Fig. 1. The 10–20 international system of electrode placement.

While sets C and D contained only activity measured during seizure free intervals, set E only contained seizure activity. Here segments were selected from all recording sites exhibiting ictal activity. All EEG signals were recorded with the same 128-channel amplifier system, using an average common reference. The data were digitized at 173.61 samples per second using 12 bit resolution. Band-pass filter settings were 0.53–40 Hz (12 dB/oct). In this study, we used two dataset (A and E) of the complete dataset. Typical EEGs are depicted in Fig. 2 (Andrzejak et al., 2001; Subasi, 2007).

5. The proposed system

5.1. Overview

The proposed hybrid identification method consists of three main parts: (i) feature extraction using Welch (FFT) method, (ii) dimensionality reduction using PCA, and (iii) EEG classification using AIRS with fuzzy resource allocation. The flow chart of the proposed method is given in Fig. 3. We explain the details of the preprocessing and classification steps in the following subsections.

5.2. Spectral analysis of EEG signals and Welch method: feature extraction

Welch method of power spectrum estimation was applied on the EEG data. Acquired EEG data was grouped in frames of 256 data points and the method was applied on these frames. Welch's method is one among the classical methods of spectrum estimation based on FFT.

FFT based Welch method is defined as classical (non-parametric) method. It is made the second modification of periodogram spectral estimator, which is to window data segments prior to computing the periodogram (Evans,

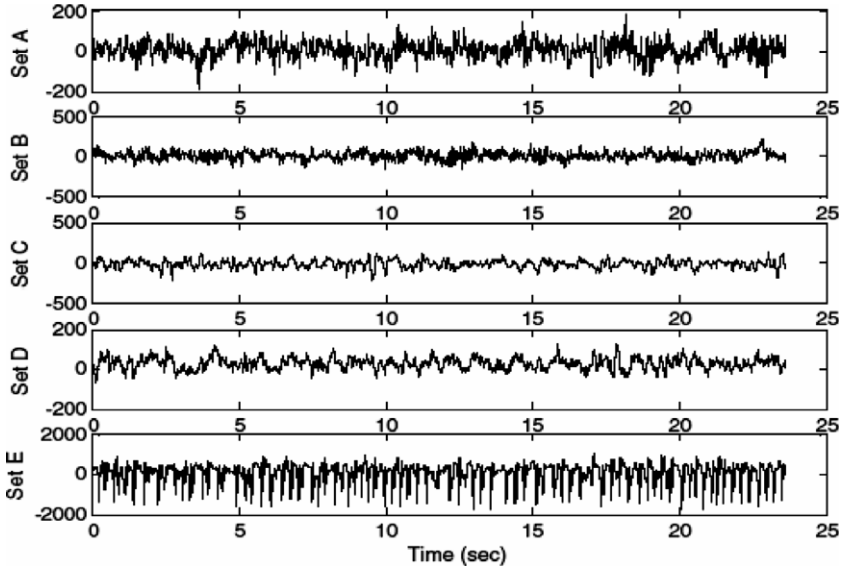

Fig. 2. Examples of five different sets of EEG signals taken from different subjects.

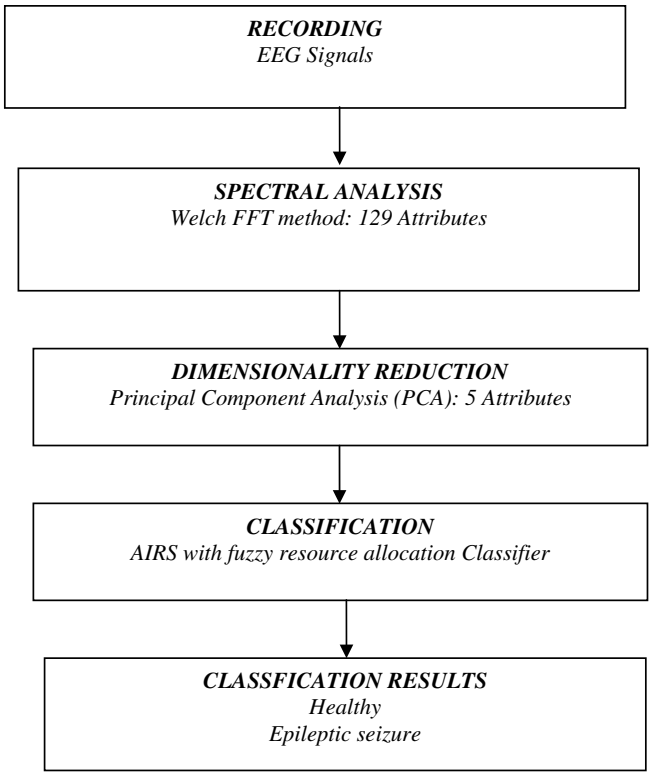

Fig. 3. The flow chart of the proposed system.

2000; Vaitkus, Cobbold, & Johnston, 1988). If available information on the signal consists of the samples $\{x(n)\}_{n=1}^{N}$, the periodogram spectral estimator is given by

$$\widehat{P}_{\mathrm{PER}}(f) = \frac{1}{N}\left|\sum_{n=1}^{N} x(n)\exp(-\mathrm{j}2\pi fn)\right|^2 \tag{1}$$

where $\widehat{P}_{\mathrm{PER}}(f)$ is the estimation of periodogram. In the Welch method, signals are divided into overlapping segments, each data segment is windowed, periodograms are calculated and then average of periodograms is found. $\{x_l(n)\}$, $l = 1,\ldots,S$ are data segments and each segment's length equals M. Note that, the overlap is often chosen to be 50%. The Welch spectrum estimate is given by

$$\widehat{P}_{\mathrm{w}}(f) = \frac{1}{S}\sum_{l=1}^{s}\widehat{P}_l(f) \quad \text{and}$$

$$\widehat{P}_l(f) = \frac{1}{M}\frac{1}{P}\left|\sum_{n=1}^{M} v(n)x_l(n)\exp(-\mathrm{j}2\pi fn)\right|^2 \tag{2}$$

where $\widehat{P}_l(f)$ is the periodogram estimate of lth segment, $v(n)$ is the data-window, P is total average of $v(n)$ and given as $P = 1/M\sum_{n=1}^{M}|v(n)|^2$, $\widehat{P}_{\mathrm{w}}(f)$ is the Welch PSD estimate, M is the length of each signal segment and S is the number of segments.

Then, evaluation of $\widehat{P}_{\mathrm{w}}(f)$ at the frequency samples basically requires the computation of the following discrete Fourier transform (DFT):

$$X(k) = \sum_{n=1}^{N} x(n)\exp\left(-\mathrm{j}\frac{2\pi}{N}\right)^{nk}, \quad k = 0,\ldots,N-1 \tag{3}$$

where $X(k)$ is expressed as the discrete Fourier coefficient, N is the length of available data and $x(n)$ is the input signal on the time domain. The procedure that computes Eq. (3) is called as FFT algorithm. The Welch PSD can be efficiently computed by the FFT algorithm. Variance of an estimator is one of the measures often used to characterize its performance. For 50% overlap and triangular window, variance for the Welch method is given by

$$\mathrm{var}(\widehat{P}_{\mathrm{w}}(f)) = \frac{9}{8S}\mathrm{var}(\widehat{P}_l(f)) \tag{4}$$

where $\widehat{P}_{\mathrm{w}}(f)$ is the Welch PSD estimate and $\widehat{P}_l(f)$ is the periodogram estimate of each signal interval (Evans, 2000; Guler, Hardalac, & Kaymaz, 2002; Vaitkus et al., 1988).

5.3. Principal component analysis (PCA): dimensionality reduction

PCA was used to make a classifier system more effective. For this aim, before classifying, PCA method was used for dimensionality reduction of EEG signals. Therefore, EEG signals dataset was represented a vector consists of 129 attributes. PCA is based on the assumption that most information about classes is contained in the directions along which the variations are the largest. The most common derivation of PCA is in terms of a standardized linear projection, which maximizes the variance in the projected space (Wang & Paliwal, 2003). For a given p-dimensional data set X, the m principal axes $T_1, T_2, \ldots, T_m$, where $1 \leqslant m \leqslant p$, are orthonormal axes onto which the retained variance is maximum in the projected space. Generally, $T_1, T_2, \ldots, T_m$ can be given by the m leading eigenvectors of the sample covariance matrix $S = (1/N)\sum_{i=1}^{N}(x_i - \mu)^{\mathrm{T}}(x_i - \mu)$, where $x_i \in X$, μ is the sample mean and N is the number of samples, so that

$$ST_i = \lambda_i T_i, \quad i \in 1,\ldots,m \tag{5}$$

where λ_i is the ith largest eigenvalue of S. The m principal components of a given observation vector $x_i \in X$ are given by

$$y = [y_1, y_2, \ldots y_m] = [T_1^{\mathrm{T}}x, T_2^{\mathrm{T}}, \ldots, T_m^{\mathrm{T}}] = T^{\mathrm{T}}x \tag{6}$$

The m principal components of x are decorrelated in the projected space. In multi-class problems, the variations of data are determined on a global basis, that is, the principal axes are derived from a global covariance matrix

$$\widehat{S} = \frac{1}{N}\sum_{j=1}^{K}\sum_{i=1}^{N_j}(x_j - \hat{\mu})(x_j - \hat{\mu})^{\mathrm{T}} \tag{7}$$

where $\hat{\mu}$ is the global mean of all the samples, K is the number of classes, N_j is the number of samples in class j; $N = \sum_{j=1}^{K}N_j$ and x_{ji} represents the ith observation from

class j. The principal axes $T_1, T_2, \ldots, T_m$ are therefore the m leading eigenvectors of $\widehat{S}$

$$\widehat{S}T_i = \hat{\lambda}_i T_i, \quad i \in 1, \ldots, m \tag{8}$$

where $\hat{\lambda}_i$ is the ith largest eigenvalue of $\widehat{S}$. An assumption made for feature extraction and dimensionality reduction by PCA is that most information of the observation vectors is contained in the subspace spanned by the first m principal axes, where $m < p$. Therefore, each original data vector can be represented by its principal component vector with dimensionality m (Lindsay, 2002).

5.4. AIRS classification algorithm: classifier system

AIRS is a resource limited supervised learning algorithm inspired from immune metaphors. In this algorithm, the used immune mechanisms are resource competition, clonal selection, affinity maturation and memory cell formation. The feature vectors presented for training and test are named as Antigens while the system units are called as B cells. Similar B cells are represented with Artificial Recognition Balls (ARBs) and these ARBs compete with each other for a fixed resource number. This provides ARBs, which have higher affinities to the training Antigen to improve. The memory cells formed after the whole training Antigens were presented are used to classify test Antigens. The algorithm is composed of four main stages, which are initialization, memory cell identification and ARB generation, competition for resources and development of a candidate memory cell, and memory cell introduction. Table 1 summarizes the mapping between the immune system and AIRS.

We give the details of our algorithm below.

1. *Initialization*: create a set of cells called the memory pool (M) and the ARB pool (P) from randomly selected training data.
2. *Antigenic presentation*: for each antigenic pattern do
   (a) *Clonal expansion*: For each element of M, determine its affinity to the antigenic pattern, which resides in the same class. Select the highest affinity memory cell (mc) and clone mc in proportion to its antigenic affinity to add to the set of ARBs (P).
   (b) *Affinity maturation*: Mutate each ARB descendant of the highest affinity mc. Place each mutated ARB into P.
   (c) *Metadynamics of ARBs*: Process each ARB using the resource allocation mechanism. This process will result in some ARB death, and ultimately controls the population. Calculate the average stimulation for each ARB, and check for termination condition.
   (d) *Clonal expansion and affinity maturation*: Clone and mutate the randomly selected subset of the ARBs left in P based on their stimulation level.
   (e) *Cycle*: While the average stimulation value of each ARB class group is less than a given stimulation threshold go to step 2c.
   (f) *Metadynamics of memory cells*: Select the highest affinity ARB of the same class as the antigen from the last antigenic interaction. If the affinity of this ARB with the antigenic pattern is better than that of the previously identified best memory cell mc then add the candidate (mc-candidate) to memory set M. If the affinity of mc and mc-candidate are below the affinity threshold, remove mc from M.
3. *Classify*: classify data items using the memory set M. Classification is performed in a k-nearest neighbor fashion with a vote being made among the k closest memory cells to the given data item being classified.

We explain each step of our algorithm in detail in the following paragraphs.

(a) *Initialization:*
The first step of the algorithm is the data pre-processing stage. In this step, the given data is normalized to ensure that the Euclidean distance between two data is in the interval of [0–1].

(b) *Memory cell identification and ARB generation:*
In this step, the algorithm iterates for each training antigen. Training antigen is presented to memory cells and the most stimulated memory cell by that antigen is cloned. The stimulation levels are calculated by Eq. (9). All of the clones with memory cell are added to ARB pool. The number of clones is determined based on the affinity between the memory cell and the antigen. Calculation of the affinity values is done by using Eq. (10), which results in higher affinities for lower Euclidean distances.

$$\text{Stimulation}(x,y) = \begin{cases} \text{affinity}(x,y), \\ \quad \text{if class of } x = \text{class of } y \\ 1 - \text{affinity}(x,y), \ \text{otherwise} \end{cases} \tag{9}$$

$$\begin{aligned} \text{affinity}(x,y) &= 1 - \text{Euclidean Distance}(x,y) \\ &= 1 - \sqrt{\sum_{i=1}^{n}(x_i - y_i)^2} \end{aligned} \tag{10}$$

Table 1
Mapping between the immune system and AIRS

Immune system	AIRS
Antibody	Feature vector
Recognition ball	Combination of feature vector and vector class
Shape-space	Type and possible values of the data vector
Clonal expansion	Reproduction of ARBs that are well matched antigens
Antigens	Training data
Affinity maturation	Random mutation of ARB and removal of the least stimulated ARBs
Immune memory	Memory set of mutated ARBs
Metadynamics	Continual removal and creation of ARBs and memory cells

(c) *Competition for resources and development of a candidate memory cell:*
In this step, the training antigen is presented to all ARBs in ARB pool. Then, all ARBs are awarded based on their resource numbers. An ARB class with higher number of resources gets higher affinity values. In other words, the assigned affinity values are proportional to the number of resources for each ARB. The required number of resources may exceed the number of resources allowed by the system. In this case, the additional resources are removed beginning with the lowest affinity ARB until the number of resources is equal to the allowed number of resources. The stimulation levels of remaining ARBs are tested and the average value of these levels is determined for each class. If any of these average values is lower than a stimulation threshold determined by the user, the ARBs belonging to that class are mutated and resulted clones are added to the ARB pool. This step proceeds until the average stimulation of all classes is bigger than the stimulation threshold. To calculate the average stimulation value for each class, we use the following expression:

$$s_i \leftarrow \frac{\sum_{j=1}^{|\mathrm{ARB}_i|} \mathrm{arb}_j.\mathrm{stim}}{|\mathrm{ARB}_i|}, \quad \mathrm{arb}_j \in \mathrm{ARB}_i \tag{11}$$

where $i = 1,\ldots,nc$, $s = \{s_1, s_2, \ldots, s_{nc}\}$, $|\mathrm{ARB}_i|$ represents the number of ARBs belonging to ith class, and arb_j.stim represents the stimulation level of jth ARB of ith class.

(d) *Memory cell introduction:*
After the total stimulation value of ARBs in all classes reaches stimulation threshold, the best ARB (i.e., ARB having the highest affinity) in the same class with training antigen is taken as a candidate memory cell. If the stimulation value between training antigen and the candidate memory cell is bigger than the stimulation value between training antigen and original memory cell selected for cloning in step 2, the candidate memory cell is added to the memory cell pool.

These steps are repeated for each training antigen. After training, test data are presented only to memory cells. k-NN algorithm is used to determine the classes in test phase. For more detailed information about AIRS, the reader is referred to Polat, Şahan, and Güneş (2006) and Watkins et al. (2001).

5.5. The parameters in AIRS classifier

One of the important advantages of AIRS is that it is not necessary to know the appropriate settings for the classifier in advance. The most important feature of the classifier is its self-determination ability (Watkins et al., 2001). The explanations of each parameter used in AIRS are given below. Table 2 summarizes these parameters.

- *Mutation rate*: a parameter between 0 and 1 that indicates the probability that any given feature (or the output) of an ARB will be mutated.
- *Affinity threshold scalar (ATS)*: a value between 0 and 1 that provides a cut-off value for memory cell replacement in the AIRS training routine when multiplied by the *affinity threshold*.
- *Stimulation threshold*: a parameter between 0 and 1 used as a stopping criterion for the training on a specific *antigen*.
- *Clonal rate*: an integer value used to determine the number of mutated clones that a given ARB is allowed to attempt to produce.
- *Number of resources*: a parameter that limits the number of ARBs allowed in the system. Each ARB is allocated to a number of resources based on its *stimulation value* and the *clonal rate*.
- *k nearest neighbor (k-NN)*: a classification scheme in which the response of the classifier to a previously unseen item is determined by a majority vote among the k closest data points.
- *k value*: the parameter that indicates how many *memory cells* should be used to determine the classification of a given test item.

5.6. Fuzzy resource allocation mechanism in AIRS classifier

The competition of resources in AIRS allows high-affinity ARBs to improve. According to this resource allocation mechanism, half of resources are allocated to the ARBs in the class of Antigen while the remaining half is distributed to the other classes. The distribution of resources is done according to a number that is found by multiplying stimulation rate with clonal rate. In the study of Marwah and Boggess, 2002, a different resource allocation mechanism was tried. In their mechanism, the Ag classes occurring more frequently get more resources. Both in classical AIRS and the study of Marwah and Boggess, resource allocation is done linearly with affinities. This linearity requires excess resource usage in the system, which results long classification time and high number of memory cells.

Table 2
Used parameters in AIRS with fuzzy resource allocation classifier for classification of EEG signals

Used parameters	For classification of EEG signals
Mutation rate	0.20
ATS (Affinity Threshold Scalar)	0.1
Stimulation threshold	0.99
Clonal rate	10
Hyper clonal rate	2.0
Iteration number	1000
K value for k-nearest neighbour	1
Number of resources in Fuzzy-AIRS	250

In this study, to get rid of this problem, resource allocation mechanism was done with fuzzy-logic. So there existed a nonlinearity because of fuzzy-rules. The difference in resource number between high-affinity ARBs and low-affinity ARBs is bigger in this method than in classical approach.

The input variable of Fuzzy resource allocation mechanism is stimulation level of ARB hence the output variable is the number of resources, which will be allocated to that ARB. As for the other fuzzy-systems, input membership functions as well as output membership functions were formed. The input membership functions are shown in Fig. 4a.

The input variable, ARB.stim, varies between 0 and 1. A membership value is calculated according to this value using input membership functions. In this calculation, two points are get which are the cutting points of membership triangles by the input value, ARB.stim. Also these points are named as membership values of input variable for related membership function. The minimum of these points is taken as the membership value of input variable x, ARB.stim (Eq. (12))

$$\mu_{A\cap B}(x) = \mathrm{Min}(\mu_A(x), \mu_B(x)), \quad x \in x \tag{12}$$

here in Eq. (1), $\mu_A(x)$ is the membership value of x in A and $\mu_B(x)$ is the membership value of x in B, where A and B are the fuzzy sets in universe X. The calculated input membership value is used to get the output value through output membership functions, which are shown in Fig. 4b.

In the x-axis of Fig. 4b, allocated resource number that will be calculated using the membership functions for the ARB is shown which changes between 0 and 10. The weight in the y-axis, which is the input membership value get as explained above, intersects the membership triangles at several points. The rule base for Fuzzy Resource Allocation is seen in Fig. 5.

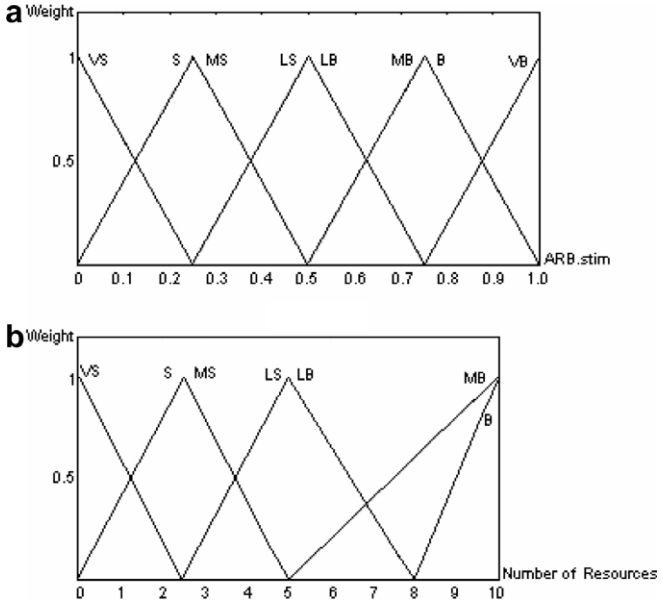

Fig. 4. (a) Input membership function and (b) output membership function.

if ARB.stim= **VS** and **S**
then Output= (**VS'** + **S'**) / 2

if ARB.stim= **S** and **MS**
then Output= (**S'** + **MS'**) / 2

if ARB.stim= **MS** and **LS**
then Output= (**MS'** + **LS'**) / 2

if ARB.stim= **LS** and **LB**
then Output= (**LS'** + **LB'**) / 2

if ARB.stim= **LB** and **MB**
then Output= (**LB'** + **MB'**) / 2

if ARB.stim= **MB** and **B**
then Output= (**MB'** + **B'**) / 2

if ARB.stim= **B** and **VB**
then Output= (**B'** + **VB'**) / 2

Fig. 5. Rule base for fuzzy resource allocation.

Table 3
Linguistic values for input and output membership functions

Input	Output
VS – very small	VS′ – very small
S – small	S′ – small
MS – middle small	MS′ – middle small
LS – little small	LS′ – little small
LB – little big	LB′ – little big
MB – middle big	MB′ – middle big
B – big	B′ – big
VB – very big	

Here VS, S, MS, etc. are the labels of input membership triangles and VS′, S′, MS′, etc. are the labels of output membership values. The rules in Fig. 5 define which points will be taken to average. For example if the input value cuts the triangles VS and S among the input membership functions, then the points to be averaged will be only the ones of VS′ and S′ triangles in the output membership functions.

Whereas determining membership value and getting output value using fuzzy-rules are of crucial importance, another important point is determination of linguistic values used in the input and output membership functions, which are shown in Table 3.

These linguistic values were determined in such a manner that the allocated resource number for ARBs which have stimulation values between 0 and 0.50 will be less while for ARBs which have stimulation values between 0.50 and 1 will be more (Polat, Şahan, Kodaz, & Güneş, 2007).

6. The experimental results

In this section, we present the performance evaluation methods used to evaluate the proposed method. Finally, we give the experimental results and discuss our observations from the obtained results.

6.1. Performance evaluation methods

We have used four methods for performance evaluation of EEG signals classification. We explain these methods in the following subsections.

6.2. Classification accuracy

In this study, the classification accuracies for the datasets are measured using Eq. (13)

$$\begin{aligned} \text{accuracy}(T) &= \frac{\sum_{i=1}^{|T|}\text{assess}(t_i)}{|T|}, \quad t_i \in T \\ \text{assess}(t) &= \begin{cases} 1, & \text{if classify}(t) = t.c \\ 0, & \text{otherwise} \end{cases} \end{aligned} \tag{13}$$

where T is the set of data items to be classified (the test set), $t \in T$, $t.c$ is the class of item t, and classify(t) returns the classification of t by AIRS.

6.3. Sensitivity and specificity

For sensitivity and specificity analysis, we use the following expressions.

$$\text{sensitivity} = \frac{\text{TP}}{\text{TP}+\text{FN}}(\%) \tag{14}$$

$$\text{specificity} = \frac{\text{TN}}{\text{FP}+\text{TN}}(\%) \tag{15}$$

where TP, TN, FP and FN denote true positives, true negatives, false positives, and false negatives, respectively.

6.4. K-fold cross-validation

K-fold cross-validation is one way to improve the holdout method. The data set is divided into k subsets, and the holdout method is repeated k times. Each time, one of the k subsets is used as the test set and the other $k-1$ subsets are put together to form a training set. Then the average error across all k trials is computed. The advantage of this method is that it is not important how the data is divided. Every data point appears in a test set exactly once, and appears in a training set $k-1$ times. The variance of the resulting estimate is reduced as k is increased. The disadvantage of this method is that the training algorithm must be rerun from scratch k times, which means it takes k times as much computation to make an evaluation. A variant of this method is to randomly divide the data into a test and training set k different times. The advantage of this method is that we can independently choose the size of the each test and the number of trials (Kohavi & Provost, 1998).

6.5. Confusion matrix

A confusion matrix (Schneider's Home Page, 2006) contains information about actual and predicted classifications done by a classification system. Performance of such a system is commonly evaluated using the data in the matrix. Table 4 shows the confusion matrix for a two class classifier.

We can explain the entries of our confusion matrix:

- a is the number of **correct** predictions that an instance is **negative**,
- b is the number of **incorrect** predictions that an instance is **positive**,
- c is the number of **incorrect** of predictions that an instance is **negative**, and
- d is the number of **correct** predictions that an instance is **positive**.

6.6. Results and discussion

The basic requirement to find an accurate model is the collection of well distributed, sufficient, and accurately measured input data. The key component of designing the classifier based on pattern classification is choice of the AIRS with fuzzy resource allocation classifier inputs, because even the best classifier will perform inadequately if the inputs are not selected well. Input selection has two meanings: (1) which components of a pattern, or (2) which set of inputs best represent a given pattern (Subasi, 2007).

We have presented power spectral density's (PSDs) of subject that has eye open and subject that has epileptic seizure subject from the EEG signals as seen Fig. 6.

The 100 EEG time series of 4096 samples for each class windowed by a rectangular window composed of 256 discrete data and then training and test sets of the classifiers were formed by 3200 vectors (1600 vectors from each class). The class distribution of the samples in the training and validation data set is summarized in Table 5.

The AIRS with fuzzy resource allocation classifier trained and tested as 50–50%, 70–30%, and 80–20%, respectively due to training and test of all the EEG signals dataset. The obtained test classification accuracies were 99.81%, 100%, and 100%, respectively. Also, we have obtained 100% classification accuracy using 10-fold cross-validation. In our experimental study, EEG signals that have eye open and epileptic seizure are classified by AIRS with fuzzy resource allocation classifier. All the obtained results were presented for 50–50% of training-test partition, 70–30% of training-test partition, and 80–20% of training-test partition in Table 6.

In this study, there were two diagnosis classes: Healthy and a patient who is subject to possible epileptic seizure. Classification results of the system were displayed by using a confusion matrix. In a confusion matrix, each cell con-

Table 4
Representation of confusion matrix

Actual	Predicted	
	Negative	Positive
Negative	a	b
Positive	c	d

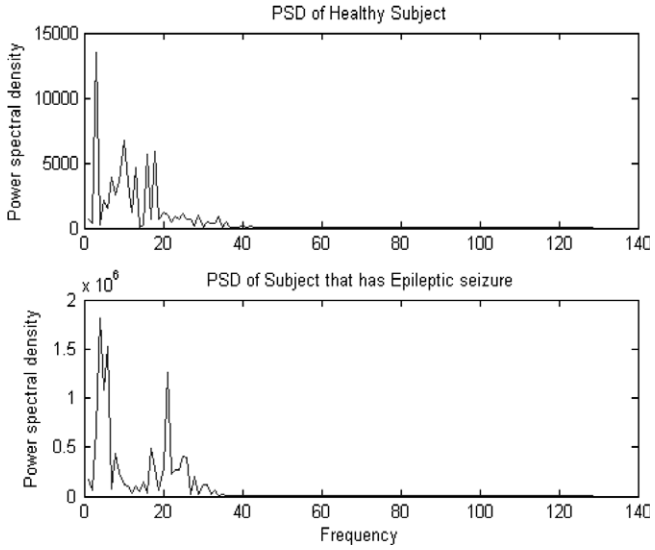

Fig. 6. Power spectral density's (PSDs) of subject that has eye open and subject that has epileptic seizure subject from the EEG signals.

Table 5
Class distribution of the samples in the training and test data sets

Class	Training set	Testing set	Total	Partition of EEG data set
Epileptic	800	800	1600	50–50% training-test partition
Normal	800	800	1600	
Total	1600	1600	3200	
Epileptic	1120	480	1600	70–30% training-test partition
Normal	1120	480	1600	
Total	2240	960	3200	
Epileptic	1280	320	1600	80–20% training-test partition
Normal	1280	320	1600	
Total	2560	640	3200	

Table 6
The obtained classification accuracy, values of sensitivity and specificity by AIRS with fuzzy resource allocation classifier for classification of EEG signals with 50–50% training-test dataset, 70–30% training-test dataset and 80–20% training-test dataset

Measures	50–50%	70–30%	80–20%	10-fold cross-validation
	Training-test partition	Training-test partition	Training-test partition	
Accuracy (%)	99.81	100	100	100
Sensitivity (%)	99.62	100	100	
Specificity (%)	100	100	100	

tains the raw number of exemplars classified for the corresponding combination of desired and actual network outputs. Table 7 gives the confusion matrix showing the classification results of this network.

Our proposed system was firstly applied to EEG signals and very promising results was obtained to classification of EEG signals. To evaluate the effectiveness of our method,

Table 7
Confusion matrix using proposed system with 50–50% training-test dataset, 70–30% training-test dataset and 80–20% training-test dataset

Output\Desired	Result (healthy)	Result (disease)	Partition of EEG data set
Result (healthy)	797	3	50–50% training-test partition
Result (disease)	0	800	
Result (healthy)	480	0	70–30% training-test partition
Result (disease)	0	480	
Result (healthy)	320	0	80–20% training-test partition
Result (disease)	0	320	

Table 8
Our method's classification accuracy for classification of EEG signals with classification accuracies obtained by other methods

Author (Year)	Method	Accuracy (%)
Guler et al. (2005)	Recurrent neural networks	96.79
Kannathal et al. (2005)	ANFIS classifier	95
Subasi (2007)	Wavelet-ME	95
Subasi (2007)	Wavelet-MLPNN	93.6
Guler and Ubeyli (2005)	Wavelet-ANFIS	98.68
Our study (2006)	Proposed system based on AIRS-PCA-FFT	100

we made experiments on the EEG signals database mentioned above. We compare our results with previous the results reported by earlier methods. Table 8 gives the classification accuracies of our method and previous methods. As we can see from these results, our method using 10-fold cross-validation obtains the highest classification accuracy, 100%, reported so far.

As can be seen from above results, we conclude that the new hybrid automated identification system based on AIRS with fuzzy resource allocation classifier, PCA, and FFT based Welch method and AIRS with fuzzy resource allocation classifier obtains very promising results in classifying the possible epileptic seizure patients. We believe that the proposed system can be very helpful to the physicians for their final decision on their patients. By using such an efficient tool, they can make very accurate decisions.

7. Conclusion and future work

In this study, AIRS with fuzzy resource allocation classifier, PCA, and FFT based Welch method based on a new hybrid automated identification system was applied to the task of classifying EEG signals and the most accurate learning methods was evaluated. Experiments were conducted on the EEG signals dataset to diagnose epileptic seizure in a fully automatic manner. The results strongly suggest that AIRS with fuzzy resource allocation classifier, PCA, and FFT based Welch method based on a new hybrid automated identification system can assist in the classification of EEG signals. We hope that more interesting results will follow on further exploration of data.

Acknowledgement

This study has been supported by Scientific Research Project of Selcuk University (Project No. 05401069).

References

Adeli, H., Zhou, Z., & Dadmehr, N. (2003). Analysis of EEG records in an epileptic patient using wavelet transform. *Journal of Neuroscience Methods, 123*(1), 69–87.

Andrzejak, R. G., Lehnertz, K., Mormann, F., Rieke, C., David, P., & Elger, C. E. (2001). Indications of nonlinear deterministic and finite-dimensional structures in time series of brain electrical activity: dependence on recording region and brain state. *Physical Review E, 64*, 061907.

Boccaletti, S., Grebogi, C., Lai, Y. C., Mancini, H., & Mazaet, D. (2000). The control of chaos: theory and applications. *Physics Report, 329*, 108–109.

De Castro, L. N., & Timmis, J. (2002). *Artificial immune systems: a new computational intelligence approach*. UK: Springer.

Duke, D., & Pritchard, W. (1991). *Measuring chaos in the human brain*. Singapore: World Scientific.

Evans, D. (2000). Doppler signal analysis. *Ultrasound in Medicine and Biology, 26*(Supplement 1), S13–S15.

Gabor, A. J., & Seyal, M. (1992). Automated interictal EEG spike detection using artificial neural networks. *Electroencephalography and Clinical Neurophysiology, 83*(5), 271–280.

Glass, L., Michel, R. G., Mackey, M., & Shrier, A. (1983). Chaos in neurobiology. *IEEE Transactions on Systems Man and Cybernetics SMC*(5), 790–798.

Glover, Jr., J. R., Raghaven, N., Ktonas, P. Y., & Frost, Jr., J. D. (1989). Context-based automated detection of epileptogenic sharp transients in the EEG: elimination of false positives. *IEEE Transactions on Biomedical Engineering, 36*(5), 519–527.

Guler, I., & Ubeyli, E. D. (2005). Adaptive neuro-fuzzy inference system for classification of EEG signals using wavelet coefficients. *Journal of Neuroscience Methods, 148*, 113–121.

Guler, N. F., Ubeyli, E. D., & Guler, I. (2005). Recurrent neural networks employing Lyapunov exponents for EEG signals classification. *Expert Systems with Applications, 29*, 506–514.

Hazarika, N., Chen, J. Z., Tsoi, A. C., & Sergejew, A. (1997). Classification of EEG signals using the wavelet transform. *Signal Processing, 59*(1), 61–72.

Jaeseung, J., Jeong-Ho, C., Kim, S. Y., & Seol-Heui, H. (2001). Nonlinear dynamical analysis of the EEG in patients with Alzheimer's disease and vascular dementia. *Clinical Neurophysiology, 18*(1), 58–67.

Jeff Schneider's Home Page, http://www.cs.cmu.edu/~schneide/tut5/node42.html (last accessed: August, 2006).

Kannathal, N., Choo, Min Lim, Rajendra Acharya, U., & Sadasivana, P. K. (2005). Entropies for detection of epilepsy in EEG. *Computer Methods and Programs in Biomedicine, 80*, 187–194.

Kohavi, R., & Provost, F. (1998). Glossary of terms. Editorial for the *Special Issue on Applications of Machine Learning and the Knowledge Discovery process*, 30 (2/3).

Lindsay, I. Smith (2002). A tutorial on principal components analysis. http://kybele.psych.cornell.edu/~edelman/Psych-465Spring-2003/PCA-tutorial.

Marwah, G., & Boggess, L. (2002) Artificial immune systems for classification: some issues. In: *Proceedings of the first international conference art. immune systems*, University of Kent at Canterbury, England (pp. 149–153).

Nigam, V. P., & Graupe, D. (2004). A neural-network-based detection of epilepsy. *Neurologial Research, 26*(1), 55–60.

Philippe, F., & Henri, K. (2001). Is there chaos in the brain? Concepts of nonlinear dynamics and methods of investigation. *Life Sciences, 324*, 773–793.

Polat, K., Şahan, S., & Güneş, S. (2006). A New method to medical diagnosis: artificial immune recognition system (AIRS) with fuzzy weighted pre-processing and application to ECG Arrhythmia (2005). *Expert Systems with Applications, 31*(2), 264–269.

Polat, K., Şahan, S., Kodaz, H., & Güneş, S. (2007). Breast cancer and liver disorders classification using artificial immune recognition system (AIRS) with performance evaluation by fuzzy resource allocation mechanism. *Expert Systems with Applications, 32*(1), 172–183.

Guler, I., Hardalac, F., & Kaymaz, M. (2002). Comparison of FFT and adaptive ARMA methods in transcranial Doppler signals recorded from the cerebral vessels. *Computers in Biology and Medicine, 32*, 445–453.

Rosso, O. A., Figliola, A., Creso, J., & Serrano, E. (2004). Analysis of wavelet-filtered tonic-clonic electroencephalogram recordings. *Medical & Biological Engineering & Computing, 42*(4), 516–523.

Şahan, S., Kodaz, H., Güneş, S., & Polat, K. (2004). A new classifier based on attribute weighted artificial immune system, *Lecture notes in computer science*, LNCS 3280, ISSN 0302-9743 (pp. 11–20).

Subasi, A. (2007). EEG signal classification using wavelet feature extraction and a mixture of expert model. *Expert Systems with Applications, 32*(4), 1084–1093.

Vaitkus, P. J., Cobbold, R. S. C., & Johnston, K. W. (1988). A comparative study and assessment of Doppler ultrasound spectral estimation techniques part II: methods and results. *Ultrasound in Medicine and Biology, 14*, 673–688.

Wang, X., & Paliwal, K. K. (2003). Feature extraction and dimensionality reduction algorithms and their applications in vowel recognition. *Pattern Recognition, The Journal of The Pattern Recognition Society, 36*, 2429–2439.

Watkins, A. (2001) AIRS: a resource limited artificial immune classifier. *Master thesis*, Mississippi State University.

Webber, W. R. S., Litt, B., Lesser, R. P., Fisher, R. S., & Bankman, I. (1993). Automatic EEG spike detection: what should the computer imitate? *Electroencephalography and Clinical Neurophysiology, 87*(6), 364–373.